JSES Open Access 3 (2019) 320–327

Contents lists available at ScienceDirect

JSES Open Access

journal homepage: www.elsevier.com/locate/jses

# An anatomical investigation into the blood supply of the proximal humerus: surgical considerations for rotator cuff repair

Natalie Keough, PhD [a], Thys de Beer, FCS SA (Orth) [b], Andre Uys, BChD, MSc [c], Erik Hohmann, MBBS, FRCS, FRCS (Tr & Orth), MD, PhD [d,e,*]

[a] Department of Anatomy, School of Medicine, Faculty of Health Sciences, University of Pretoria, Pretoria, South Africa
[b] Life Groenkloof Hospital, Pretoria, South Africa
[c] Department of Oral Pathology and Oral Biology, School of Dentistry, Faculty of Health Sciences, University of Pretoria, Pretoria, South Africa
[d] Department of Orthopaedic Surgery and Sports Medicine, Valiant Clinic/Houston Methodist Group, Dubai, United Arab Emirates
[e] School of Medicine, University of Pretoria, Pretoria, South Africa

ARTICLE INFO

*Keywords:*
Humeral head
blood supply
anterior circumflex humeral artery
posterior circumflex humeral artery
rotator cuff repair

*Level of evidence:* Anatomy Study; Cadaveric Dissection

**Background:** The purpose of this study was to investigate the blood supply of the humeral head (HH) originating from the anterior (ACHA) and posterior circumflex humeral arteries (PCHA).
**Methods:** Formalin preserved specimens were used to measure ACHA length, ACHA length in the bicipital groove (BG), the length of the ascending branch of the ACHA, the penetration point of the ascending branch of the ACHA at the greater tuberosity (GT), and the penetration point of the ascending branch PCHA at the GT. Fresh specimens were used to identify the intraosseous vascular network by both the ACHA and PCHA by injecting a contrast medium using a high-resolution microfocus computed tomography. Specimens were then dissected to expose where the branches of the ACHA and PCHA penetrate the bone, and a small section of the medial head was removed to visualize dye penetration of the cancellous bone.
**Results:** Seven variations for the course of the ACHA were observed. In 36%, the ACHA runs posterior to the BG and posterior to the long head of biceps tendon, and splits into the anterolateral ascending and descending branch. The ascending branch enters the medial wall of the GT. Microfocus computed tomography demonstrated that the intraosseous branch of the ascending branch of the ACHA runs within the GT in a medial direction from its penetration point just along the lateral edge of the BG. Intraosseous accumulation of contrast within the GT supply occurs more toward the inferior aspect of the HH, and the anterior-superior and superior-medial aspect of the HH is not perfused. This region is a high-risk zone for avascular necrosis.
**Conclusion:** The results of this study suggest that 7 variations for the course of the ACHA exist. These variations and the interruption of the intraosseous arterial network in the GT with surgery and suture anchor placement result in a high-risk zone in the superomedial aspect of the humeral head overlapping with the area where early aseptic necrosis is identified.


Arthroscopic treatment for symptomatic rotator cuff (RC) tears has become standard treatment. Arthroscopic suture anchor placement, and specifically the use of multiple anchors (>4), has been suggested as a cause of damage to the intraosseous arteries and network within the greater tuberosity (GT), which may lead to reduced healing of the tendon-bone construct and also carries a risk of avascular necrosis (AVN) of the humeral head (HH).[8] The incidence of reported AVN after arthroscopic RC repair using anchors is increasing, and over the last 2 decades, 20 cases have been reported.[2,4,6,7,11,15,16,18]

Based on earlier research, branches from the anterior circumflex humeral artery (ACHA) are the main blood supply to the HH,[10,13,16] but other researchers suggested that the posterior circumflex humeral artery (PCHA) may also contribute more toward the vascularization of the proximal humerus.[3,8] Lambert[17] suggested that the PCHA is of more importance to articular segment and tuberosity perfusion than the ACHA. Regardless of the contribution of blood supply to the HH, both of these arteries' intraosseous components and networks are potentially at risk during anchor placement.

The study was approved by the Research Ethics Committee of the Faculty of Health Sciences, University of Pretoria (70/2017) and all research complies with the National Health Act 63 of 2003.

* Corresponding author: Erik Hohmann, MBBS, FRCS, FRCS (Tr & Orth), MD, PhD, Valiant Clinic/Houston Methodist, 13th street, City Walk, Dubai, United Arab Emirates.
*E-mail address:* ehohmann@houstonmethodist.org (E. Hohmann).

https://doi.org/10.1016/j.jses.2019.09.002

Previous authors have also suggested that AVN is potentially caused by direct damage to the ascending branch of the ACHA, and suture anchor placement could be one of the contributing factors.[2,7,11] In contrast, Kim et al[15] surveyed 12 centers to collect cases with rapid progressive HH osteonecrosis after arthroscopic RC repair with suture anchors and suggested that anchor placement could not be the single cause. The authors proposed that surgeons should be more aware of a potentially higher risk of AVN in elderly females with dominant side involvement.[15] Interestingly, of the 20 reported cases with AVN after arthroscopic repair, 65% had an additional extra-articular biceps tenotomy, 70% were reported female, and all cases involved the dominant extremity.[2,6,7,11,15,18]

Close proximity of the ACHA to the intra-articular part of the long head of biceps tendon (LHBT) could be one of the contributing factors that may result in bone ischemia or even AVN by direct or indirect damage to the ascending branch of the ACHA when either performing a biceps tenotomy or tenodesis or placing anterior suture anchors. Therefore, the purpose of this study was to investigate the blood supply of the HH originating from the ACHA and PCHA. It was hypothesized that the vascular supply to the HH would receive contributions from both the ACHA and PCHA, but contributions are variable and no definite pattern can be identified.

## Methods

To increase the numbers of specimens a combination of fresh frozen and formaline preserved specimens was used. The fresh frozen specimens were acquired from Department of Anatomy, School of Medicine, Faculty of Health Sciences, University of Pretoria, South Africa. The formalin preserved cadaveric specimens were obtained from the Department of Anatomy. These specimens were resected from cadavers before they were used during the basic anatomy courses offered at the department. This study had 2 arms. Anatomic variations and morphology of the ACHA and PCHA were investigated in embalmed cadavers. The intraosseous vascular network for the ACHA and PCHA was then investigated in fresh anatomic specimens.

### *Embalmed cadaveric specimens*

A total of 87 cadaveric shoulders from 25 males (25 left and 25 right) and 21 females (20 left and 17 right) were used in this study (age range: 56-95 years; mean: 77.5). Standard dissection techniques were used to expose the branches of both the ACHA and the PCHA. The skin and muscle envelope was carefully removed, the axillary artery was identified in the axilla, and the blood vessels were traced from the origin toward the humerus. These branches were then analyzed for origin and course.

The following measures for the both ACHA and PCHA were taken (Table I):

[1] ACHA length: the length from its origin until the most medial crest of the bicipital groove (BG) (Fig. 1).
[2] ACHA length in the BG: the length within the BG between the most medial and most lateral crests of the groove (which was the portion that lies deep to the long head biceps tendon (Fig. 1).
[3] Ascending branch length: the length of the ascending branch of the ACHA from its origin to the most lateral crest of the BG to the point where the branch enters the medial aspect of the GT (Fig. 1).
[4] Ascending branch penetration point to the lateral aspect of the GT: the distance from the point where the ascending branches penetrate the medial aspect of the GT to the most superolateral point of the GT (Figs. 1 and 2).
[5] PCHA ascending branch penetration point to the lateral aspect of the GT: the distance from the PCHA's ascending branch penetration into the GT to the most superolateral point of the GT (Fig. 2).

The measures were taken by the chief investigator using a calibrated Vernier caliper. The arm was abducted to 20°, the measures were repeated 3 times, and the results averaged. If one of the measures deviated more than 10% from the average, the measures were repeated for this variable. As the purpose of this project was to investigate the blood supply of the HH, intra- and interclass correlations were not deemed necessary and these measures are for descriptive purposes only.

### *Fresh specimens*

Ten adult (age range: 67-83 years; mean: 76) fresh specimens were used in this study. These specimens were used to identify the intraosseous vascular network by both the ACHA and PCHA by injecting a contrast medium. For this purpose, 5 specimens were dissected to expose the axillary artery, which were then cannulated with 5.0 mm plastic tubing. The specimens were then infused with 100 mL 10% barium sulfate solution containing a 3% gelatin mix.[21] The upper limb was then cooled in a refrigerator at 12°C for 20 minutes to allow the infusion to set. The specimens were then scanned with a high-resolution cone beam computed tomography (CBCT) machine. The data were volume rendered in 3D and the blood vessels visualized using Ez3D Plus software (VATECH global, Hwaseong-si, Gyeonggi-do, South Korea). The remaining 5 specimens were dissected to bone to expose the foramina where the branches of the ACHA and PCHA penetrate the bone at and around the GT and articular surface of the HH. These 5 shoulder specimens were then infused with 100 mL blue-dyed 10% barium sulfate solution containing a 3% gelatin mix through direct injection into the visible foramina of the branches of the PCHA (spread along the lateral aspect of the GT) as well as the major entry foramen of the ascending branch of the ACHA (lateral edge of the BG below the

**Table I**
Measurements for the anterior circumflex humeral artery (ACHA) and its branches in relation to the greater tuberosity (GT) as well as the PCHA ascending branch into the GT

| Measurement (mm) | Description |
|---|---|
| 1. ACHA length | Length of the ACHA from its origin till the most medial crest of the bicipital groove (Fig. 2) |
| 2. ACHA length in the bicipital groove | Length of the ACHA between the most medial and most lateral crests of the bicipital groove; the portion of the ACHA that lies deep to the long head tendon of biceps brachii (Fig. 2) |
| 3. Ascending branch length | Length of the ascending branch of the ACHA from its origin at the most lateral crest of the bicipital groove to the point where this vessel enters the medial aspect of the GT (Fig. 2) |
| 4. Ascending branch penetration point to the lateral aspect of GT (lp-GT) | Distance from the point where the ascending branches penetrate the medial aspect of the GT to the most lateral point of the GT (lp-GT) (Figs. 2 and 3) |
| 5. PCHA ascending branch penetration point to the lateral aspect of GT (lp-GT) | Distance from the PCHA's ascending branch (PCHA-b) penetration into the GT to the most superolateral point of the GT (lp-GT) (Fig. 3) |

*PCHA*, posterior circumflex humeral artery.

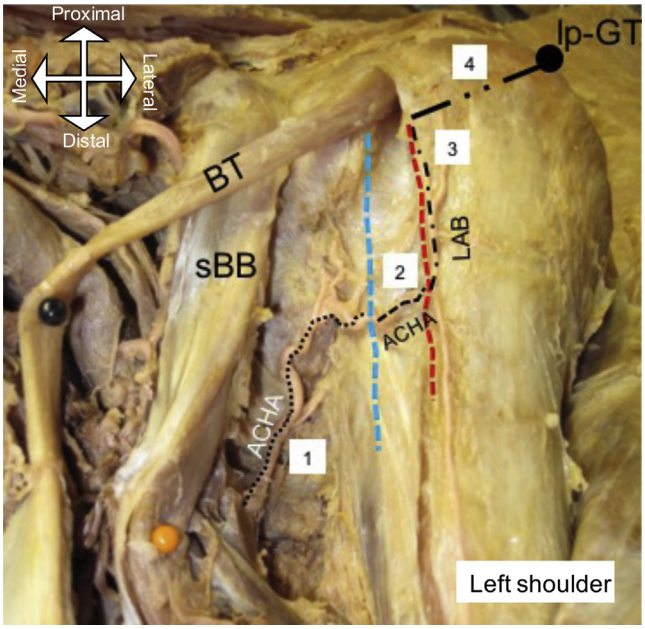


**Figure 1** (1) Length of the anterior circumflex humeral artery (ACHA) from the point of origin to the medial ridge/crest (-------) of the bicipital groove (BG); (2) length of ACHA in the BG (deep to the long head of the biceps tendon); (3) length of the lateral ascending branch (LAB) of the ACHA along the lateral ridge/crest (-------) till penetration into the greater tuberosity; (4) distance from LAB penetration into the greater tuberosity to the most superolateral point of the greater tuberosity (lp-GT). *BT*, biceps tendon; *sBB*, short head of biceps.

transverse humeral ligament) and the distribution to the exposed HH noted and photographed. The specimens were then cooled to allow the infusion to set. Afterward, the specimens were scanned in a high-resolution CBCT machine. The high-resolution data were volume rendered in 3D and the blood vessels visualized using Ez3D Plus software (VATECH global).

### *Statistical analysis*

The demographic variables for both the embalmed and fresh cadaveric specimens were reported using descriptive statistics. For the embalmed specimens, the numeric parameters measured included the length and distances as described in the Methods section in millimeters. The mean length, standard deviations, and 95% confidence intervals were calculated, and Fisher's exact test of independence was used to determine significant differences between sex and side. Variations in the origin of both the ACHA and PCHA and branching patterns of the ACHA were described using frequencies and percentages. For the fresh specimens, observations of the intraosseous blood supply were recorded in a qualitative manner. All analyses were conducted using STATA SE (Version 12.0; StataCorp, College Station, TX, USA) for Windows.

## Results

### *Cadaveric results*

The ACHA and PCHA were most commonly observed to originate as separate branches (ACHA = 76%; PCHA = 60%) from the axillary

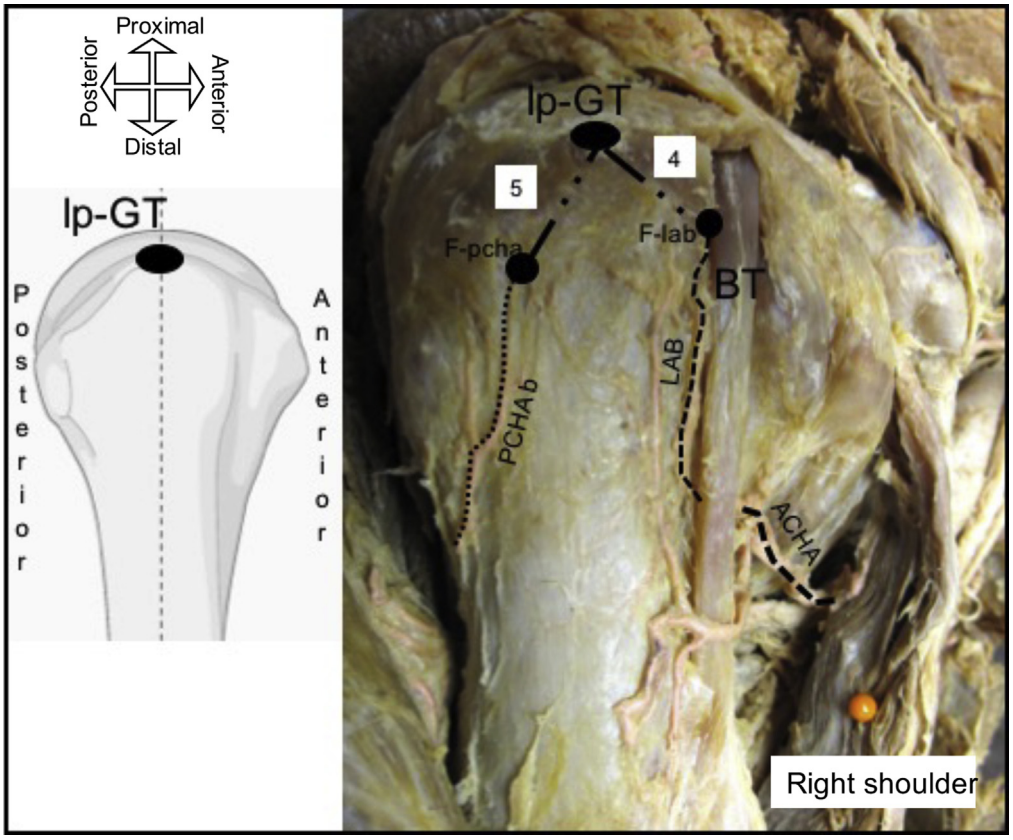


**Figure 2** Lateral view of the proximal humerus illustrating measurement: (4) distance from LAB penetration into the greater tuberosity to the most superolateral point of the greater tuberosity (lp-GT) and (5) distance from the posterior circumflex humeral artery's ascending branch (PCHAb) penetration into the greater tuberosity to the most superolateral point of the greater tuberosity (lp-GT). *BT*, biceps tendon; *F-lab*, foramen of the lateral ascending branch (LAB) of the anterior circumflex humeral artery (ACHA); *F-pcha*, foramen of the branch of the posterior circumflex humeral artery.

**Table II**
Origin of the anterior circumflex humeral artery

| Sex | Side | 1 | 2 | 3 | Total | Fischer's exact *P* value |
|---|---|---|---|---|---|---|
| Male | L | 20 | 5 | 0 | 25 | .7019 |
| | R | 21 | 3 | 1 | 25 | |
| Female | L | 14 | 6 | 0 | 20 | .8490 |
| | R | 11 | 5 | 1 | 17 | |
| Male total | L+R | 41 | 8 | 1 | 50 | .2625 |
| Female total | L+R | 25 | 11 | 1 | 37 | |
| Sample total | M+F | 66 | 19 | 2 | 87 | |

1: separate, 2: common trunk, 3: subscapular artery.

artery (Tables II and III). No statistical significant difference was noted between the male and female measurements or between left and right sides; therefore, all measurements for the 5 parameters measured were pooled together, and the results are presented in Table IV. While observing the course of the ACHA, it was noted that 7 distinct patterns of variation exist. The most common pattern was variation 1 (18/50) where the ACHA courses to the medial edge of the BG, runs posterior to the LHBT crossing the floor of the grove, in a horizontal fashion, toward the lateral edge of the groove, and then splits into an ascending and descending branch. The least common patterns were variations 5 and 6 (1/50). These variations and their descriptions are presented in Table V.

*Fresh specimen results*

Fig. 3 illustrates axial and coronal CBCT images taken from the fresh specimens, which clearly indicates the intraosseous branch of the ascending branch of the ACHA coursing within the GT, in a medial direction, from its penetration point just along the lateral edge of the BG. This point was situated just beneath the transverse humeral ligament, which had to be cut to gain access to the foramen.

Fig. 4 illustrates the axial and coronal sections of one of the fully dissected fresh specimens that were dissected to the bone, exposing the foramina through which the branches of the ACHA and PCHA enter the GT; the blue-dyed barium-sulfate solution was injected directly into these foramina. These foramina were variable and spread along the lateral aspect of the GT. These images in Fig. 4 (*A-D*) illustrate the intraosseous accumulation of contrast within the GT and the medial migration of this arterial network supply toward the more inferior aspect of the HH. Fig. 5 clearly demonstrates that the superior aspect of the HH is not accumulating contrast, which suggests that this location is a potential high-risk zone (HRZ) for necrosis. When defining the HH as a circle and dividing it into 3 equal parts similar to a pie chart with 1 segment representing the anterior-inferior third, 1 segment representing the posterior-inferior third, and 1 segment representing the superior third, this zone is located at the superior third. These findings were observed on all 5 fresh specimens. Further dissection by removing the medial aspect of the HH supports the micro-CT findings (Fig. 6). There is obvious distribution of the blue dye inferior aspect of the HH and moderate dye observed in the superior-posterior aspect, but the anterior-superior and superior-medial aspect (HRZ) of the HH obviously lacks perfusion. Figs. 5 and 6 clearly demonstrate that the superior aspect of the HH is not accumulating contrast, which suggests that this location is a potential HRZ for necrosis. These findings were observed on all 5 fresh specimens. This area correlates with the origins and position of developing AVN.

**Table III**
Origin of the posterior circumflex humeral artery

| Sex | Side | 1 | 2 | 3 | Total | Fischer's exact *P* value |
|---|---|---|---|---|---|---|
| Male | L | 16 | 5 | 4 | 25 | .4724 |
| | R | 14 | 3 | 7 | 24 | |
| Female | L | 13 | 6 | 1 | 20 | .4354 |
| | R | 8 | 5 | 3 | 16 | |
| Male total | L+R | 30 | 8 | 11 | 49 | .1858 |
| Female total | L+R | 21 | 11 | 4 | 36 | |
| Sample total | M+F | 51 | 19 | 15 | 85 | |

**Table IV**
Measurements (in millimeter) for the anterior circumflex humeral artery and its branches in relation to the greater tuberosity (GT) as well as the PCHA ascending branch into the GT

| Measurement | Sex | Side | N | Mean | SD | 95% CI | *P* value |
|---|---|---|---|---|---|---|---|
| 1 | M | L | 19 | 40.9 | 6.18 | 37.9-43.8 | .1785 |
| | | R | 17 | 37.2 | 9.63 | 32.3-42.2 | |
| | F | L | 14 | 41.9 | 6.81 | 37.9-45.8 | .0397 |
| | | R | 12 | 36.9 | 4.16 | 34.3-39.6 | |
| | M | L+R | 36 | 39.1 | 8.08 | 36.4-41.9 | .2726 |
| | F | L | 14 | 41.9 | 6.81 | 37.9-45.8 | |
| | M | L+R | 36 | 39.1 | 8.08 | 36.4-41.9 | .3716 |
| | F | R | 12 | 36.9 | 4.16 | 34.3-39.6 | |
| 2 | M | L | 20 | 10.3 | 2.26 | 9.2-11.4 | .3956 |
| | | R | 16 | 11.2 | 3.93 | 9.1-13.3 | |
| | F | L | 14 | 11.7 | 7.87 | 7.2-16.3 | .2472 |
| | | R | 12 | 8.9 | 1.72 | 7.8-10.0 | |
| | M | L+R | 36 | 10.7 | 3.10 | 9.7-11.8 | .1456 |
| | F | L+R | 26 | 10.4 | 5.96 | 8.0-12.8 | |
| 3 | M | L | 20 | 25.2 | 7.39 | 21.7-28.7 | .7623 |
| | | R | 16 | 26.1 | 6.02 | 22.9-29.3 | |
| | F | L | 14 | 23.3 | 5.01 | 20.5-26.2 | .5255 |
| | | R | 12 | 22.2 | 3.33 | 20.1-24.4 | |
| | M | L+R | 36 | 25.6 | 6.73 | 23.3-27.9 | .0197 |
| | F | L+R | 26 | 22.8 | 4.27 | 21.1-24.6 | |
| 4 | M | L | 22 | 19.7 | 3.01 | 18.4-21.0 | .8327 |
| | | R | 19 | 19.9 | 2.60 | 18.6-21.1 | |
| | F | L | 13 | 19.5 | 3.49 | 17.4-21.6 | .7956 |
| | | R | 12 | 19.9 | 3.50 | 17.7-22.1 | |
| | M | L+R | 41 | 19.8 | 2.79 | 18.9-20.7 | .9197 |
| | F | L+R | 25 | 19.7 | 3.43 | 18.3-21.1 | |
| 5 | M | L | 20 | 13.1 | 3.08 | 11.6-14.5 | .4543 |
| | | R | 16 | 13.2 | 2.49 | 11.8-14.5 | |
| | F | L | 10 | 12.8 | 1.99 | 11.4-14.3 | .2109 |
| | | R | 9 | 14.2 | 2.59 | 12.2-16.2 | |
| | M | L+R | 26 | 13.1 | 2.80 | 12.2-14.1 | .2088 |
| | F | L+R | 19 | 13.5 | 2.33 | 12.4-14.6 | |

*PCHA*, posterior circumflex humeral artery; *SD*, standard deviation; *CI*, confidence interval.

## Discussion

The most important finding of this study was that 7 possible variations exist for the course of the ACHA when using the long head biceps tendon as a reference. The most common pattern was observed in 36% of the cadaver specimens where the ACHA courses to the medial edge of the BG; runs posterior to the LHBT, in a horizontal fashion, crossing the floor of the groove toward the lateral edge of the BG, and then splits into the ascending branch and descending branch; the ascending branch courses superiorly where it enters the medial wall of the GT just beneath the transverse humeral ligament. The 2 least common variations were observed in 1% of the cadaver specimens: in variation 5, the ACHA courses to the medial edge of the BG, courses anterior to the LHBT in a horizontal fashion toward the lateral edge of the BG, and then splits into the ascending and descending branch; the ascending branch courses superiorly where it enters the medial wall of the GT. In variation 6, the ACHA splits into the ascending and descending branches before reaching the medial edge of the BG; these 2 branches run anterior to the LHBT in a horizontal fashion toward the lateral edge of the BG, and then the ascending anterolateral branch courses superiorly to enter the medial wall of the GT.

**Table V**
Descriptions of the 7 variations observed for the branching pattern of the anterior circumflex humeral artery

| Variation | Description | Prevalence (/50) |
|---|---|---|
| 1 | ACHA courses to the medial edge of the BG and runs posterior to the LHBT crossing the floor of the groove toward the lateral edge of the BG; here it splits into the anterolateral (ascending) and descending branch; the anterolateral branch courses superiorly where it enters the medial wall of the GT | N = 18/50 (36%) |
| 2 | ACHA courses to the medial edge of the BG and splits into the anterolateral (ascending) and descending branches; these branches run posterior to the LHBT crossing the floor of the BG in a horizontal fashion toward the lateral edge of the BG; at the lateral edge, the anterolateral branch courses superiorly to enter the medial wall of the GT | N = 14/50 (28%) |
| 3 | ACHA courses to the medial edge of the BG and splits into the anterolateral (ascending) and descending branches; the anterolateral branch then courses directly, in an oblique fashion, posterior to the LHBT, crossing the floor of the BG to enter the medial wall of the GT; the descending branch continues posterior to the LHBT in a horizontal fashion toward the lateral edge of the BG | N = 5/50 (10%) |
| 4 | ACHA splits into the anterolateral (ascending) and descending branches before it reaches the medial edge of the BG; these 2 branches run posterior to the LHBT crossing the floor to the BG in a horizontal fashion toward the lateral edge of the BG; at the lateral edge, the anterolateral branch courses superiorly to enter the medial wall of the GT | N = 2/50 (4%) |
| 5 | ACHA courses to the medial edge of the BG; it then courses anterior to the LHBT in a horizontal fashion toward the lateral edge of the BG; here it splits into the anterolateral (ascending) and descending branches; the anterolateral branch courses superiorly where it enters the medial wall of the GT | N = 1/50 (2%) |
| 6 | ACHA splits into the anterolateral (ascending) and descending branches before it reaches the medial edge of the BG; these 2 branches run anterior to the LHBT in a horizontal fashion toward the lateral edge of the BG; at the anterolateral edge, the anterolateral branch courses superiorly to enter the medial wall of the GT | N = 1/50 (2%) |
| 7 | ACHA splits into the anterolateral (ascending) and descending branches before it reaches the medial edge of the BG; the anterolateral branch runs anterior to the LHBT in an oblique fashion to the entry point on the medial wall of the GT; the descending branch runs posterior to the LHBT in a horizontal fashion toward the lateral edge of the BG | N = 9/50 (18%) |

*ACHA*, anterior circumflex humeral artery; *BG*, bicipital groove; *LHBT*, long head of biceps tendon; *GT*, greater tuberosity.

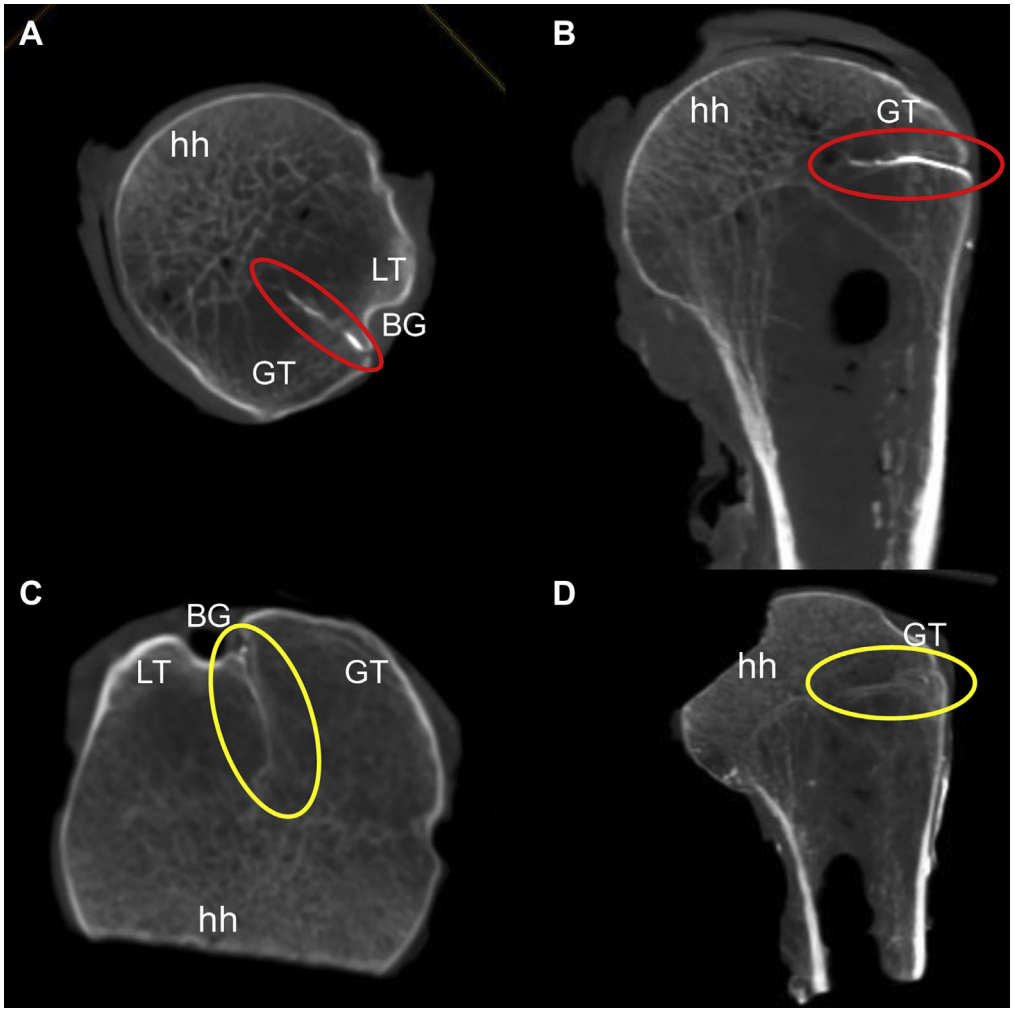


**Figure 3** (**A** and **B**) Axial and coronal microfocus-CT views of the proximal humerus of individual 1, clearly showing the arcuate artery's (◯) entrance into the superolateral aspect of the bicipital groove (BG) and its intraosseous course into the greater tuberosity (GT) with its medially migration toward the humeral head (hh); (**C** and **D**) Axial and coronal microfocus-CT views of the proximal humerus of individual 2, clearly showing the arcuate artery's (◯) entrance into the superolateral aspect of the BG and its intraosseous course into the GT with its medial migration toward the hh. *CT*, computed tomography; *LT*, lesser tubercle.

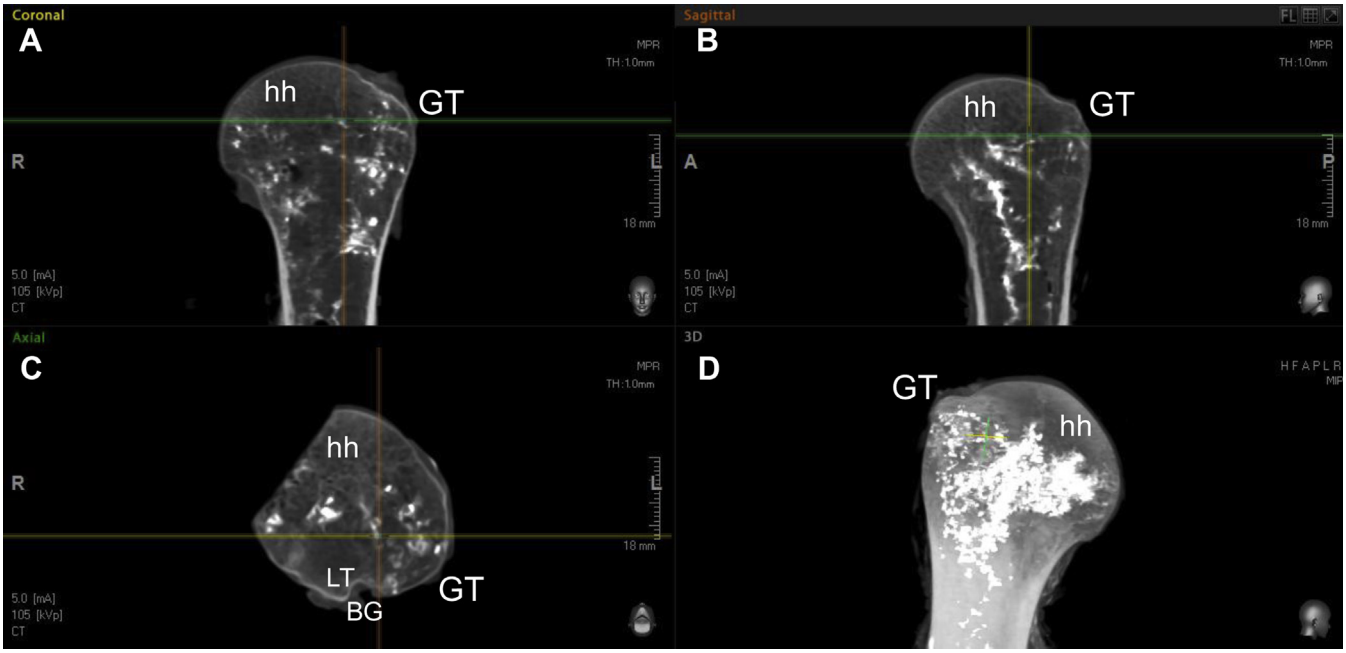


**Figure 4** (**A** and **B**) Coronal and sagittal sections of the proximal humerus indicating the accumulation of intraosseous supply in the greater tuberosity (GT) with medial migration of the supply to the inferomedial aspect of the humeral head (hh); (**C**) axial view of the proximal hh indicating the intraosseous vessels in the GT and medial migration to the hh; (**D**) 3D rendering of the proximal hh demonstrating the intraosseous supply from the GT toward the inferomedial aspect of the hh. *BG*, bicipital groove; *LT*, lesser tubercle.

The proximal humerus and HH are supplied by intraosseous branches originating from both the ACHA and PCHA.[5,8,13] The origin of the ACHA has been described as arising as a separate branch from the axillary artery approximately 1 cm distal to the inferior border of the pectoralis major; however, this can vary from direct branching from a common trunk, giving rise to both the PCHA and the ACHA, or as a branch of the subscapular artery.[1,5,20]

In this study, a separate origin for both the ACHA (73%) and PCHA (64%) was observed and only 27% showed origins from a common trunk. These results support previous findings by Duparc et al[8] but contradicted Meyer et al,[19] who found that the 67% of their sample showed a common origin trunk for the ACHA and PCHA from the axillary artery. These differences highlight the variations of blood supply and that both the ACHA and PCHA play important roles. The variability has potential implications for fractures of the proximal humerus but should also be considered with RC repair, suture anchor placement, and surgery to the LHBT.

The PCHA has a posterior course through the quadrangular space and gives off terminal branches, one toward the teres minor and deltoid, and another that runs toward the upper humeral epiphysis to enter the HH at the bone cartilage border with a few branches extending to the GT.[8,13,19] These branches extend to the epiphysis contributing blood supply to the rest of the glenohumeral joint capsule (inferior, posterior, and superior) as well as the posterior and superior parts of the GT.[8] In the current study, branches extending to the lateral aspect of the GT were noted, and these branches entered the bone approximately 13 mm inferior to the most lateral point of the GT. These branches essentially contribute to the anastomotic connections with the intraosseous contributions from the ACHA within the GT itself, forming the network that distributes blood to the HH. Extraosseous connection between the 2 circumflex arteries was not observed as previously described by Duparc et al[8]; only the well-defined anterolateral ascending and descending branches were observed. These branches vascularize the HH, and preservation may be critical during surgery. Duparc et al[8] used colored latex and selectively injected it into the origins of the ACHA and PCHA using embalmed cadavers. Both injection solution and the use of embalmed specimens could explain the differences, but it is most likely just the anatomic variability similar to the variations that were described for the ACHA in this project.

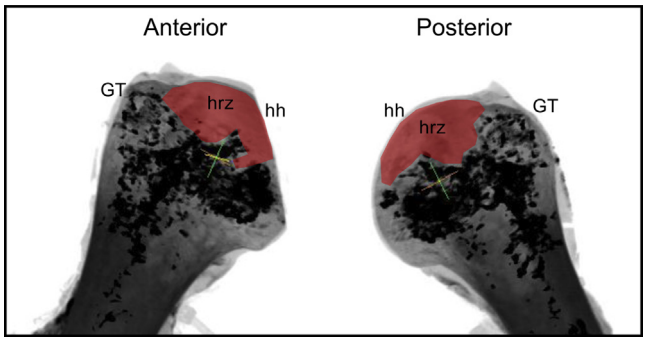


**Figure 5** Microfocus-CT image of the proximal humerus indicating the accumulation of intraosseous blood vessels in the greater tuberosity (GT) and the medial migration of supply to the more inferomedial aspect of the humeral head (hh); the high-risk zone (hrz, red fill) also evident on the superior aspect of the hh. *CT*, computed tomography.

The rate of AVN of proximal humerus fractures has been reported to be 10%-33%.[1,22] The blood supply to the HH is complex, and variations with regard to the anatomy of the ACHA suggest a more significant contribution from the PCHA to the epiphysis via its perforation at the anatomical neck. In this study, the intraosseous branches of the arcuate artery and the PCHA were observed to accumulate within the GT traversing medially toward the HH. These intraosseous vessels were especially well defined in the common positions used for suture-anchor placement in the bone during arthroscopic repair. The intraosseous anastomotic networks served the majority of the HH except for a small region on the most superomedial aspect of the head. This region overlaps considerably with the area where aseptic necrosis of the HH usually begins.[4,12] Based on the observations, it is possible that this area is an HRZ. This zone receives a more indirect and reduced supply from the

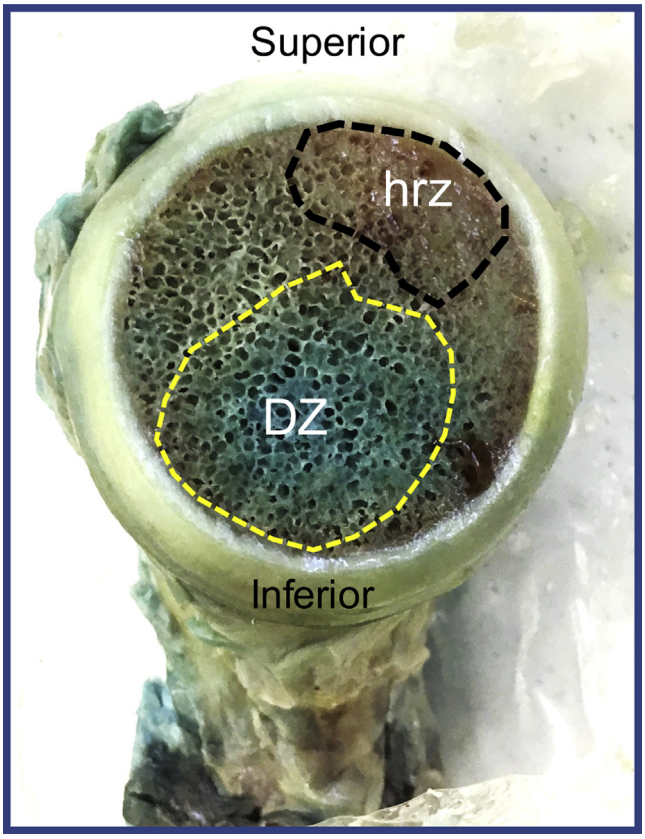


**Figure 6** Medial view of the humeral head indicating the densely-supplied zone (DZ) in the inferior region of the head with the high-risk zone (hrz) along the more superior aspect of the humeral head.

surrounding intraosseous vessels. If the intraosseous vessels are damaged during suture-anchor placement in the GT, this area may be at a higher risk of interrupted or complete loss of blood flow, resulting in aseptic necrosis. However, the contribution of the intraosseous blood supply to the HRZ is not clearly understood. It is also quite possible that any form of compromise to their points of origin may have effects on their terminal areas of distribution.

However, the findings of this suggest that there may be a possible link between specific variations of the ACHA and the incidence of postarthroscopic AVN. This assumption clearly needs to be investigated further to establish the possible relationship between anatomic variations in blood supply and high-risk areas where AVN could occur if anchors are placed in the watershed zone between the ACHA and PCHA intraosseous blood supply. AVN could be caused by either suture anchor placement or due to biceps pulley lesions and biceps tenodesis surgery disrupting the blood supply from the ACHA. Perhaps the combination of the existence of the HRZ and the interruption of the intraosseous arterial network in the GT with surgery, the variation in ACHA course in relation to the biceps tendon, and the patient being female with dominant side involvement may all be strong contributing factors toward the development of postarthroscopic AVN of the HH.

### *Limitations*

This study has several limitations. Preservation of human specimens with formalin could result in changes in functional anatomy, and handling during dissection could be more difficult.[9] However, Kennel et al[14] demonstrated no significant differences between soft embalming and formalin, and it is unlikely that embalming influenced either dissection or tissue handling. As with any cadaveric study, the mean age of the donor was relatively old and changes with age could have influenced blood supply when injecting the intraosseous vascular network with a contrast medium.

## Conclusion

The results of this study suggest that 7 variations for the course of the ACHA exist.

These variations and the interruption of the intraosseous arterial network in the GT with surgery and suture anchor placement result in a HRZ in the superomedial aspect of the HH overlapping with the area where early aseptic necrosis is identified.

## Disclaimer

This research was funded by the National Research Foundation, South Africa (NRF; grant number 105920). Any opinions, findings, and conclusions expressed in this article are those of the authors, and therefore, the NRF does not accept any liability in regard thereto. These authors, their immediate family, and any research foundation with which they are affiliated did not receive any financial payments or other benefits from any commercial entity related to the subject of this article.

## References

1. Archer LA, Furey A. Rate of avascular necrosis and time to surgery in proximal humerus fractures. Musculoskelet Surg 2016;100:213–6. https://doi.org/10.1007/s12306-016-0425-0.
2. Beauthier V, Sanghavi S, Roulot E, Hardy P. Humeral head osteonecrosis following arthroscopic rotator cuff repair. Knee Surg Sports Traumatol Arthrosc 2010;18:1432–4. https://doi.org/10.1007/s00167-009-1016-5.
3. Brooks CH, Revell WJ, Heatley FW. Vascularity of the humeral head after proximal humeral fractures. J Bone Joint Surg 1993;75:132–6.
4. Byun JW, Shim JH, Shin WJ, Cho SY. Rapid progressive atypical atraumatic osteonecrosis of humeral head: a case report. Korean J Anaesthesiol 2014;66:398–401. https://doi.org/10.4097/kjae.2014.66.5.398.
5. Chen YX, Zhu Y, Wu FH, Zheng X, Wangyang YF, Yuan H, et al. Anatomical study of simple landmarks for guiding the quick access to humeral circumflex arteries. BMC Surg 2014;14:39. https://doi.org/10.1186/1471-2482-14-39.
6. Cho HI, Cho HL, Hwang TH, Wang TH, Cho H. Rapidly progressive osteonecrosis of the humeral head after arthroscopic Bankart and rotator cuff repair in a 66-year old woman: a case report. Clin Shoulder Elbow 2015;18:167–71. https://doi.org/10.5397/cise.2015.18.3.167.
7. Dilisio MF, Noble JS, Bell RH, Noel CR. Postarthroscopic humeral head osteonecrosis treated with reverse shoulder arthroplasty. Orthopedics 2013;36:e377–80. https://doi.org/10.3928/01477447-20130222-30.
8. Duparc F, Muller JM, Fréger P. Arterial blood supply of the proximal humeral epiphysis. Surg Radiol Anat 2001;23:185–90.
9. Eisma R, Lamb C, Soames RW. From formalin to Thiel embalming: What changes? One anatomy department's experiences. Clin Anat 2013;26:564–71. https://doi.org/10.1002/ca.22222.
10. Gerber C, Schneeberger AG, Vinh TS. The arterial vascularization of the humeral head: an anatomical study. J Bone Joint Surg Am 1990;72:1486–94.
11. Goto M, Gotoh M, Mitsui Y, Okawa T, Higuchi F, Nagata K. Rapid collapse of the humeral head after arthroscopic rotator cuff repair. Knee Surg Sports Traumatol Arthrosc 2015;23:514–6. https://doi.org/10.1007/s00167-013-2790-7.
12. Hasan SS, Romeo AA. Nontraumatic osteonecrosis of the humeral head. J Shoulder Elbow Surg 2002;11:281–98. https://doi.org/10.1067/mse.2002.124347.
13. Hettrich CM, Boraiah S, Dyke JP, Neviaser A, Helfet DL, Lorich DG. Quantitative assessment of the vascularity of the proximal part of the humerus. J Bone Joint Surg Am 2010;92:943–8. https://doi.org/10.2106/JBJS.H.01144.
14. Kennel L, Martin DMA, Shaw H, Wilkinson T. Learning anatomy through Thiel- vs. formalin-embalmed cadavers: student perceptions of embalming methods and effects on functional anatomy knowledge. Anat Sci Educ 2018;11:166–74. https://doi.org/10.1002/ase.1715.
15. Kim JK, Jeong HJ, Shin SJ, Yoo JC, Rhie TY, Park KJ, et al. Rapid progressive osteonecrosis of the humeral head after arthroscopic rotator cuff surgery. Arthroscopy 2018;34:41–7. https://doi.org/10.1016/j.arthro.2017.06.051.

16. Laing PG. The arterial supply of the adult humerus. J Bone Joint Surg 1956;38A:1105–16.
17. Lambert SM. Ischaemia, healing and outcomes in proximal humerus fractures. EFORT Open Rev 2018;3:304–15. https://doi.org/10.1302/2058-5241.3.180005.
18. Magee TH, Gaenslen ES, Seitz R, Hinson GA, Wetzel LH. MR imaging of the shoulder after surgery. AJR Am J Roentgenol 1997;168:925–8.
19. Meyer C, Alt V, Hassanin H, Heiss C, Stahl JP, Giebel G, et al. The arteries of the humeral head and their relevance in fracture treatment. Surg Radiol Anat 2005;27:232–7. https://doi.org/10.1007/s00276-005-0318-7.
20. Parada SA, Dilisio MF, Kennedy CD. Management of complications after rotator cuff surgery. Curr Rev Musculoskeletal Med 2015;8:40–52. https://doi.org/10.1007/s12178-014-9247-6.
21. Qiu X, Shi X, Quyang J, Xu D, Zhao D. A method to quantify and visualize the femoral head introaosseous arteries by micro-CT. J Anat 2016;229:326–33. https://doi.org/10.1111/joa.12475.
22. Xu J, Zhang C, Wang T. Avascular necrosis in proximal humerus fractures in patients treated with operative fixation: a meta-analysis. J Orthop Res Surg 2014;9:31. https://doi.org/10.1186/1749-799X-9-31.